REAL TIME FLIGHT DYNAMICS MODEL IDENTIFICATION OF TILT-ROTOR AIRCRAFT

Wu Wei, scorpio_nuaa@nuaa.edu.cn, Nanjing University of Aeronautics and Astronautics (China)

Abstract
An improved real time identification method for tilt-rotor aircraft flight dynamics modeling is developed in this paper. A general parametric flight dynamics model which can be used for online identification purpose in all 3 flight modes is established, and an unideal noise model is also built in order to minimize the influences to the identification accuracy caused by measurement noise. An adaptive model structure identification algorithm is established by introducing local accuracy criteria, so that the time variant optimal model structure can be obtained in real time. A weighted recursive least squares algorithm is established for parameter identification, and a time variant weighting matrix is designed to provide best numerical performance of the identification procedure at any time. A comprehensive nonlinear flight dynamics model of a sample tilt-rotor aircraft is used to build a numerical simulation platform and identification results of the sample aircraft in fixed wing mode, helicopter model as well as transition mode are obtained based on simulation flight test. Finally, the flight dynamics model of an unmanned tilt-rotor aircraft in helicopter mode is identified by using the real flight test data. The identification results show that the real time identification method for tilt-rotor aircraft developed in this paper is effective, efficient and robust.

1. INTRODUCTION

The tilt-rotor aircraft is a special aircraft which combines the advantages of both fixed wing aircraft and rotorcraft. It is also one of the promising configurations for high speed and heavy lift helicopters[1-3]. However, a tilt-rotor aircraft is also more complicated than conventional fixed wing aircraft and rotorcraft. It has 3 different flight modes, and the dynamic characteristic of each mode is different. In fixed wing mode, the tilt-rotor aircraft is weak coupled and the rotor is working in propeller mode, which means there is no flapping motion. However, in helicopter mode, a tilt-rotor aircraft is highly coupled, and the rotor flapping dynamics cannot be ignored anymore. In transition mode, the pylon tilting movement increases the complexity of the aerodynamic environment. At the meantime, the position of the center of gravity (C.G.) and the moment of inertia of the aircraft keep changing during transition flight.

The complexities of a tilt-rotor aircraft bring many difficulties in flight control system design[4-6] as well as flying quality analysis and design[7]. One of the difficulties is lack of accurate flight dynamics model. However, due to the complicated dynamic behaviour of a tilt-rotor aircraft, it is still a challenging work to build flight dynamics model with high accuracy for such aircraft by using theoretical methods[8]. System identification, as one of the modern modeling technique, is an effective tool to increase the modeling confidence of complex system. It has been firstly applied in fixed wing aircraft flight dynamics modeling since 1950s, and great success was made at early time. However, many difficulties were encountered when trying to apply system identification technique to rotorcraft flight dynamics modeling. These problems arose from many factors, such as the rotorcraft is a typical high order and highly coupled system and the quality of test data are usually poorer than fixed wing aircraft due to high level of measurement noise. Currently, there are many excellent methods that solved the system identification problem for conventional rotorcraft well in both time domain and frequency domain[9-11]. Moreover, in order to increase the identification accuracy and robustness, many new identification methods that based on modern system identification theory have been developed for both fixed wing aircraft and helicopters in recent years[12-14]. For tilt-rotor aircraft, there are also many excellent works related to nonparametric and parametric identification problems have been done based on the flight test data of XV-15[15-18]. Besides offline system identification, there are also many research works concentrate on real

Presented at 44th European Rotorcraft Forum, Delft, The Netherlands, 19-20 September, 2018

time identification technique. Recursive least squares algorithm and Kalman filter are the most commonly used methods for online system identification[19-22].

Although great achievements have been obtained in aircraft system identification during the past decades, difficulties are still remained in identifying complex aircraft such as tilt-rotor aircraft. The current identification method for tilt-rotor aircraft is used for offline system identification purpose[18]. However, in some applications such as adaptive control system design, a real time identification module is required. Previous research works related to tilt-rotor aircraft system identification were concentrated on helicopter mode (hover) and fixed wing mode (cruise flight), the identification problem in transition mode has not been investigated yet. However, the real time identification will be carried out in all flight modes. The current online identification methods are usually applied to simple models. However, a tilt-rotor aircraft is a typical high order system, and the model structure may also be time variant since there are 3 different flight modes. Therefore, it is difficult to use current methods directly to identify such complex model. Moreover, the high level of measurement noise of tilt-rotor aircraft in helicopter mode and transition model will contaminate the flight data heavily, the influences of unideal noise must be considered during identification process. However, in current methods, the noise is usually treated as white noise, and a biased estimation of model parameters may obtained based on this assumption.

In order to solve the above problems, an improved real time identification method for tilt-rotor aircraft flight dynamics modeling is developed in this paper. A general parametric flight dynamics model is established for all 3 flight modes, and an unideal noise model is also introduced to decrease the identification inaccuracy caused by measurement noise. Then local identification accuracy criteria are introduced to replace the overall criteria in model structure determination procedure. An adaptive model structure identification algorithm is then established. Finally, an improved online parameter estimation method which combines real time model structure determination and modified weighted recursive least squares algorithm is developed. The developed real time identification method is firstly applied to identify a tilt-rotor aircraft flight dynamics model in all 3 flight modes based on a nonlinear tilt-rotor aircraft simulation program. Then, the flight dynamics model of an unmanned tilt-rotor aircraft is identified based on the real flight test data in helicopter mode.

2. A GENERAL PARAMETRIC MODEL FOR REAL TIME IDENTIFICATION

A tilt-rotor aircraft has 3 different flight modes and the dynamic characteristic in each flight mode is different. However, in order to implement real time identification, a general parametric model for all flight modes is required. A linear time variant state space model is used in this paper, as shown in Eq. (1).

(1) $$\dot{\boldsymbol{x}}(t)=\boldsymbol{A}(t)\boldsymbol{x}(t)+\boldsymbol{B}(t)\boldsymbol{u}(t)+\boldsymbol{\varepsilon}(t)$$

Where, $\boldsymbol{x}$ is state vector, $\boldsymbol{u}$ is control input vector, $\boldsymbol{A}$ is stability matrix, $\boldsymbol{B}$ is control matrix, $\boldsymbol{\varepsilon}$ is noise vector.

In fixed wing flight mode, the rotor works like a propeller, and it does not flap. Therefore, a rigid body flight dynamics model is sufficient in this mode, and then the $\boldsymbol{A}$ and $\boldsymbol{B}$ matrix can be written as Eq. (2) and Eq. (3)

(2) $$\boldsymbol{A}=\begin{bmatrix} X_u & X_v & X_w & X_p & X_q-w_0(t) & X_r+v_0(t) & 0 & -g\cos\theta_0(t) \\ Y_u & Y_v & Y_w & Y_p+w_0(t) & Y_q & Y_r-u_0(t) & g\cos\theta_0(t)\cos\varphi_0(t) & -g\sin\theta_0(t)\sin\varphi_0(t) \\ Z_u & Z_v & Z_w & Z_p-v_0(t) & Z_q+u_0(t) & Z_r & -g\cos\theta_0(t)\sin\varphi_0(t) & -g\sin\theta_0(t)\cos\varphi_0(t) \\ L_u & L_v & L_w & L_p & L_q & L_r & 0 & 0 \\ M_u & M_v & M_w & M_p & M_q & M_r & 0 & 0 \\ N_u & N_v & N_w & N_p & N_q & N_r & 0 & 0 \\ 0 & 0 & 0 & 1 & 0 & \tan\theta_0(t) & 0 & 0 \\ 0 & 0 & 0 & 0 & 1 & 0 & 0 & 0 \end{bmatrix}$$

Presented at 44th European Rotorcraft Forum, Delft, The Netherlands, 19-20 September, 2018

(3)
$$\boldsymbol{B}=\begin{bmatrix} X_{\delta_{long}} & X_{\delta_{lat}} & X_{\delta_{col}} & X_{\delta_{ped}} \\ Y_{\delta_{long}} & Y_{\delta_{lat}} & Y_{\delta_{col}} & Y_{\delta_{ped}} \\ Z_{\delta_{long}} & Z_{\delta_{lat}} & Z_{\delta_{col}} & Z_{\delta_{ped}} \\ L_{\delta_{long}} & L_{\delta_{lat}} & L_{\delta_{col}} & L_{\delta_{ped}} \\ M_{\delta_{long}} & M_{\delta_{lat}} & M_{\delta_{col}} & M_{\delta_{ped}} \\ N_{\delta_{long}} & N_{\delta_{lat}} & N_{\delta_{col}} & N_{\delta_{ped}} \\ 0 & 0 & 0 & 0 \\ 0 & 0 & 0 & 0 \end{bmatrix}$$

It should be noticed that in this model, the trim values of attitude and velocities in body axis are time variant. The reason is in real time identification, the airspeed of the aircraft varies at a wide range. However, the linear model is valid only in a small range around baseline state. In practice, several baseline states are defined, and discrete trim values are used instead of continues function for convenient.

In helicopter flight mode, the rotor flapping dynamics should be introduced. This is because the rotor flapping motion has large influences on the phase of frequency response. A simplified rotor flapping equation as shown in Eq. (4) is used in this paper.

(4)
$$\begin{cases} \tau_f \dot{\beta}_{1s} = -\beta_{1s} + Lf_{\beta_{1c}}\beta_{1c} + \tau_f p + Lf_{\delta_{long}}\delta_{long} + Lf_{\delta_{lat}}\delta_{lat} \\ \tau_f \dot{\beta}_{1c} = -\beta_{1c} + Mf_{\beta_{1s}}\beta_{1s} + \tau_f q + Mf_{\delta_{long}}\delta_{long} + Mf_{\delta_{lat}}\delta_{lat} \end{cases}$$

In which, β_{1s} is lateral flapping angle, β_{1c} is longitudinal flapping angle, and τ_f is rotor flapping time constant.
Then the stability matrix and control matrix in helicopter flight mode can be found in Eq. (5) and Eq. (6).

(5)
$$\boldsymbol{A}=\begin{bmatrix} X_u & X_v & X_w & X_p & X_q - w_0(t) & X_r + v_0(t) & 0 & -g\cos\theta_0(t) & X_{\beta_{1s}} & X_{\beta_{1c}} \\ Y_u & Y_v & Y_w & Y_p + w_0(t) & Y_q & Y_r - u_0(t) & g\cos\theta_0(t)\cos\varphi_0(t) & -g\sin\theta_0(t)\sin\varphi_0(t) & Y_{\beta_{1s}} & Y_{\beta_{1c}} \\ Z_u & Z_v & Z_w & Z_p - v_0(t) & Z_q + u_0(t) & Z_r & -g\cos\theta_0(t)\sin\varphi_0(t) & -g\sin\theta_0(t)\cos\varphi_0(t) & Z_{\beta_{1s}} & Z_{\beta_{1c}} \\ L_u & L_v & L_w & L_p & L_q & L_r & 0 & 0 & L_{\beta_{1s}} & L_{\beta_{1c}} \\ M_u & M_v & M_w & M_p & M_q & M_r & 0 & 0 & M_{\beta_{1s}} & M_{\beta_{1c}} \\ N_u & N_v & N_w & N_p & N_q & N_r & 0 & 0 & N_{\beta_{1s}} & N_{\beta_{1c}} \\ 0 & 0 & 0 & 1 & 0 & \tan\theta_0(t) & 0 & 0 & 0 & 0 \\ 0 & 0 & 0 & 0 & 1 & 0 & 0 & 0 & 0 & 0 \\ 0 & 0 & 0 & 1 & 0 & 0 & 0 & 0 & -\frac{1}{\tau_f} & \frac{Lf_{\beta_{1c}}}{\tau_f} \\ 0 & 0 & 0 & 0 & 1 & 0 & 0 & 0 & \frac{Mf_{\beta_{1s}}}{\tau_f} & -\frac{1}{\tau_f} \end{bmatrix}$$

Presented at 44th European Rotorcraft Forum, Delft, The Netherlands, 19-20 September, 2018

(6)
$$\boldsymbol{B}=\begin{bmatrix} X_{\delta_{long}} & X_{\delta_{lat}} & X_{\delta_{col}} & X_{\delta_{ped}} \\ Y_{\delta_{long}} & Y_{\delta_{lat}} & Y_{\delta_{col}} & Y_{\delta_{ped}} \\ Z_{\delta_{long}} & Z_{\delta_{lat}} & Z_{\delta_{col}} & Z_{\delta_{ped}} \\ L_{\delta_{long}} & L_{\delta_{lat}} & L_{\delta_{col}} & L_{\delta_{ped}} \\ M_{\delta_{long}} & M_{\delta_{lat}} & M_{\delta_{col}} & M_{\delta_{ped}} \\ N_{\delta_{long}} & N_{\delta_{lat}} & N_{\delta_{col}} & N_{\delta_{ped}} \\ 0 & 0 & 0 & 0 \\ 0 & 0 & 0 & 0 \\ \frac{Lf_{\delta_{long}}}{\tau_f} & \frac{Lf_{\delta_{lat}}}{\tau_f} & 0 & 0 \\ \frac{Mf_{\delta_{long}}}{\tau_f} & \frac{Mf_{\delta_{lat}}}{\tau_f} & 0 & 0 \end{bmatrix}$$

In transition flight mode, besides rotor flapping, the pylon tilting motion changes the directions of rotor forces, C.G. position and moment of inertia of the aircraft. The consequence is the total forces and moments at C.G. position changes with different tilting angle. Considering that the tilting angle is controlled by pilot, it is not a free state, so the tilting angle should be treated as control input. Therefore, in transition flight mode, the stability matrix is the same as in helicopter flight mode. However, the control matrix now is extended as Eq. (7). The last column in Eq. (7) is control derivative vector of tilting angle input.

(7) $$\boldsymbol{B}=\begin{bmatrix} X_{\delta_{long}} & X_{\delta_{lat}} & X_{\delta_{col}} & X_{\delta_{ped}} & X_{\beta_p} \\ Y_{\delta_{long}} & Y_{\delta_{lat}} & Y_{\delta_{col}} & Y_{\delta_{ped}} & Y_{\beta_p} \\ Z_{\delta_{long}} & Z_{\delta_{lat}} & Z_{\delta_{col}} & Z_{\delta_{ped}} & Z_{\beta_p} \\ L_{\delta_{long}} & L_{\delta_{lat}} & L_{\delta_{col}} & L_{\delta_{ped}} & L_{\beta_p} \\ M_{\delta_{long}} & M_{\delta_{lat}} & M_{\delta_{col}} & M_{\delta_{ped}} & M_{\beta_p} \\ N_{\delta_{long}} & N_{\delta_{lat}} & N_{\delta_{col}} & N_{\delta_{ped}} & N_{\beta_p} \\ 0 & 0 & 0 & 0 & 0 \\ 0 & 0 & 0 & 0 & 0 \\ \frac{Lf_{\delta_{long}}}{\tau_f} & \frac{Lf_{\delta_{lat}}}{\tau_f} & 0 & 0 & 0 \\ \frac{Mf_{\delta_{long}}}{\tau_f} & \frac{Mf_{\delta_{lat}}}{\tau_f} & 0 & 0 & 0 \end{bmatrix}$$

It is apparently that in all flight modes, the linear state space flight dynamics model of tilt-rotor aircraft can all be written in Eq. (1). The stability matrix and control matrix in different flight modes will be submatrix of Eq. (5) and Eq. (7). Therefore, a general flight dynamics model for real time identification can be written as Eq. (8).

(8) $\dot{\boldsymbol{x}}_w(t)=\boldsymbol{A}_w(t)\boldsymbol{x}_w(t)+\boldsymbol{B}_w(t)\boldsymbol{u}_w(t)+\boldsymbol{\varepsilon}_w(t)$

Where, the weighted state vector, control vector, noise vector, stability matrix and control matrix are defined as Eq. (9) ~ Eq.(13)

(9) $\boldsymbol{x}_w=\begin{bmatrix}\boldsymbol{W}_x^1\boldsymbol{x}_1\\ \boldsymbol{W}_x^2\boldsymbol{x}_2\end{bmatrix}$,

$$\boldsymbol{x}_1=[u,v,w,p,q,r,\varphi,\theta]^T,\ \boldsymbol{x}_2=[\beta_{1s},\beta_{1c}]^T$$

(10) $\boldsymbol{u}_w=\begin{bmatrix}\boldsymbol{W}_u^1\boldsymbol{u}_1\\ W_u^2u_2\end{bmatrix}$

$$\boldsymbol{u}_1=\left[\delta_{long},\delta_{lat},\delta_{col},\delta_{ped}\right]^T,u_2=\beta_p$$

(11) $\boldsymbol{\varepsilon}_w=\begin{bmatrix}\boldsymbol{W}_\varepsilon^1\boldsymbol{\varepsilon}_1\\ \boldsymbol{W}_\varepsilon^2\boldsymbol{\varepsilon}_2\end{bmatrix}$

(12) $\boldsymbol{A}_w=\begin{bmatrix}\boldsymbol{W}_A^{11}\boldsymbol{A}_{11} & \boldsymbol{W}_A^{12}\boldsymbol{A}_{12}\\ \boldsymbol{W}_A^{21}\boldsymbol{A}_{21} & \boldsymbol{W}_A^{22}\boldsymbol{A}_{22}\end{bmatrix}$

(13) $\boldsymbol{B}_w=\begin{bmatrix}\boldsymbol{W}_B^{11}\boldsymbol{B}_{11} & \boldsymbol{W}_B^{12}\boldsymbol{B}_{12}\\ \boldsymbol{W}_B^{21}\boldsymbol{B}_{21} & \boldsymbol{0}_{2\times1}\end{bmatrix}$

In Eq. (12), matrix $\boldsymbol{A}_{11}$, $\boldsymbol{A}_{12}$, $\boldsymbol{A}_{21}$ and $\boldsymbol{A}_{22}$ are submatrix of Eq. (5). In Eq. (13), $\boldsymbol{B}_{11}$, $\boldsymbol{B}_{12}$, and $\boldsymbol{B}_{21}$ are submatrix of Eq. (7).

In fixed wing flight mode, the values of each weighting matrix can be found in Eq. (14)

(14) $$\begin{cases}\boldsymbol{W}_x^1=\boldsymbol{W}_\varepsilon^1=\boldsymbol{I}_{8\times8},\boldsymbol{W}_x^2=\boldsymbol{W}_\varepsilon^2=\boldsymbol{0}_{2\times2}\\ \boldsymbol{W}_u^1=\boldsymbol{I}_{4\times4},W_u^2=0\\ \boldsymbol{W}_A^{11}=\boldsymbol{I}_{8\times8},\boldsymbol{W}_A^{12}=\boldsymbol{0}_{8\times8},\boldsymbol{W}_A^{21}=\boldsymbol{W}_A^{22}=\boldsymbol{0}_{2\times2}\\ \boldsymbol{W}_B^{11}=\boldsymbol{I}_{8\times8},\boldsymbol{W}_B^{12}=\boldsymbol{0}_{8\times8},\boldsymbol{W}_B^{21}=\boldsymbol{0}_{2\times2}\end{cases}$$

Presented at 44th European Rotorcraft Forum, Delft, The Netherlands, 19-20 September, 2018

Similarly, the values of each matrix in helicopter flight mode and transition flight mode can be found in Eq. (15) and (16) respectively.

$$(15)\quad \begin{cases} \boldsymbol{W}_x^1=\boldsymbol{W}_\varepsilon^1=\boldsymbol{I}_{8\times8},\boldsymbol{W}_x^2=\boldsymbol{W}_\varepsilon^2=\boldsymbol{I}_{2\times2} \\ \boldsymbol{W}_u^1=\boldsymbol{I}_{4\times4},W_u^2=1 \\ \boldsymbol{W}_A^{11}=\boldsymbol{I}_{8\times8},\boldsymbol{W}_A^{12}=\boldsymbol{I}_{8\times8},\boldsymbol{W}_A^{21}=\boldsymbol{W}_A^{22}=\boldsymbol{I}_{2\times2} \\ \boldsymbol{W}_B^{11}=\boldsymbol{I}_{8\times8},\boldsymbol{W}_B^{12}=\boldsymbol{0}_{8\times8},\boldsymbol{W}_B^{21}=\boldsymbol{I}_{2\times2} \end{cases}$$

$$(16)\quad \begin{cases} \boldsymbol{W}_x^1=\boldsymbol{W}_\varepsilon^1=\boldsymbol{I}_{8\times8},\boldsymbol{W}_x^2=\boldsymbol{W}_\varepsilon^2=\boldsymbol{I}_{2\times2} \\ \boldsymbol{W}_u^1=\boldsymbol{I}_{4\times4},W_u^2=1 \\ \boldsymbol{W}_A^{11}=\boldsymbol{I}_{8\times8},\boldsymbol{W}_A^{12}=\boldsymbol{I}_{8\times8},\boldsymbol{W}_A^{21}=\boldsymbol{W}_A^{22}=\boldsymbol{I}_{2\times2} \\ \boldsymbol{W}_B^{11}=\boldsymbol{I}_{8\times8},\boldsymbol{W}_B^{12}=\boldsymbol{I}_{8\times8},\boldsymbol{W}_B^{21}=\boldsymbol{I}_{2\times2} \end{cases}$$

3. IMPROVED ONLINE IDENTIFICATION METHOD

In real time identification, one difficult problem is the flight state of the aircraft may vary in a wide range and there will be no time invariant trim state. Therefore, a fixed or general optimal model structure which is used in offline identification does not exist. However, in current online identification methods, constant simple model structures are commonly used. Such constant model structures may decrease the accuracy of parameter estimation. Another difficult problem is the collected flight state data are usually contaminated by measurement noise. In offline identification, a comprehensive data processing procedure is applied before model identification. However, in real time identification, it is impossible to carry out such procedure. So the influences of noise to identification accuracy must be considered. In current online identification methods, white noise assumption is commonly used. However, the real measurement noise is always colored. Therefore, the white noise assumption may bring a bias in parameter estimation. In order to solve the above problems, an adaptive model structure determination method and an improved online parameter estimation algorithm with colored noise model are developed in this paper.

3.1. Adaptive model structure detemination

The general model structure of tilt-rotor aircraft can be changed in different flight modes according to Eq. (8) ~ Eq. (16). In each flight mode, a real time model structure determination procedure can be implemented based on numerical analysis. The main idea is to calculate local Cramer-Rao bound and Insensitivity function in real time, and then a cost function based on these two criteria can be established for each parameter. Finally, the model structure is adjusted according to the value of cost function.

The local Cramer-Rao bound and Insensitivity function for each parameter can be defined as Eq. (17) and (18) respectively.

$$(17)\quad \boldsymbol{CR}_i=\sqrt{(\boldsymbol{H}^{-1})_{ii}}$$

$$(18)\quad \boldsymbol{IS}_i=\sqrt{(\boldsymbol{H}_{ii})^{-1}}$$

Where, $\boldsymbol{H}$ is local Hessian matrix, as defined in Eq. (19)

$$(19)\quad \boldsymbol{H}_{ij}^t=\left(\frac{\partial \boldsymbol{v}^t}{\partial \boldsymbol{\theta}_i^t}\right)^T \boldsymbol{R}^{-1}\frac{\partial \boldsymbol{v}^t}{\partial \boldsymbol{\theta}_j^t}$$

In which, $\boldsymbol{v}$ is model prediction error as defined in Eq. (20), $\boldsymbol{\theta}$ is model parameter vector to be identified, $\boldsymbol{R}$ is error covariance matrix.

It should be noticed that, the error vector and model parameter vector are all real time values in Eq. (19). However, the covariance matrix $\boldsymbol{R}$ which can be written as Eq. (21) will be average value in a time sequence with length L.

$$(20)\quad \boldsymbol{v}^t=\boldsymbol{x}_w^t-\boldsymbol{x}_{measure}^t$$

$$(21)\quad \boldsymbol{R}=\frac{1}{L}\sum_{t=t_0}^{t_0+(L-1)\Delta t}\boldsymbol{v}^t\bullet(\boldsymbol{v}^t)^T$$

The partial derivatives in Eq. (19) can be obtained by solving the parameter sensitivity equation as written in Eq. (22).

$$(22)\quad \frac{d}{dt}\left(\frac{\partial \boldsymbol{x}_w}{\partial \boldsymbol{\theta}}\right)=\boldsymbol{A}_w\frac{\partial \boldsymbol{x}_w}{\partial \boldsymbol{\theta}}+\frac{\partial \boldsymbol{A}_w}{\partial \boldsymbol{\theta}}\boldsymbol{x}_w+\frac{\partial \boldsymbol{B}_w}{\partial \boldsymbol{\theta}}\boldsymbol{u}_w$$

The cost function for real time model structure identification can be defined as Eq. (23).

$$(23)\quad J_i=\frac{\boldsymbol{CR}_{critical}-\boldsymbol{CR}_i}{\boldsymbol{CR}_{critical}}+\frac{\boldsymbol{IS}_{critical}-\boldsymbol{IS}_i}{\boldsymbol{IS}_{critical}}$$

Where, $\boldsymbol{CR}_{critical}$ and $\boldsymbol{IS}_{critical}$ are critical values of Cramer-Rao bound and Insensitivity function respectively.

It is apparently that in Eq. (17) ~ Eq. (23), every vectors and matrix are local variables except covariance matrix $\boldsymbol{R}$. In order to increase the computational efficiency of Hessian matrix, which is very important in real time identification, a recursive calculation of inverse matrix $\boldsymbol{R}^{-1}$ is required. Therefore, the recursive formula of $\boldsymbol{R}^{-1}$ can be derived as follows.
Assume:

$$\boldsymbol{V}_{t-1}=\sum_{t=t_0}^{t_0+(L-2)\Delta t}\boldsymbol{v}^t\bullet(\boldsymbol{v}^t)^T,$$

$t_c=t_0+(L-1)\Delta t$ is current time, then,

Presented at 44th European Rotorcraft Forum, Delft, The Netherlands, 19-20 September, 2018

$$
\begin{aligned}
\boldsymbol{R}_t^{-1} &= \left(\frac{1}{L}\sum_{t=t_0}^{t_0+(L-1)\Delta t} \boldsymbol{v}^t \bullet (\boldsymbol{v}^t)^T\right)^{-1} \\
&= \left(\frac{1}{L}\sum_{t=t_0}^{t_0+(L-2)\Delta t} \boldsymbol{v}^t \bullet (\boldsymbol{v}^t)^T + \frac{1}{L}\boldsymbol{v}^{t_c} \bullet (\boldsymbol{v}^{t_c})^T\right)^{-1} \quad (24)\\
&= L\left(\boldsymbol{V}_{t-1} + \boldsymbol{v}^{t_c} \bullet (\boldsymbol{v}^{t_c})^T\right)^{-1}
\end{aligned}
$$

According to matrix inversion lemma, Eq. (24) can be written as:

$$\boldsymbol{R}_t^{-1} = L\left[\boldsymbol{V}_{t-1}^{-1} - \boldsymbol{V}_{t-1}^{-1}\boldsymbol{v}^{t_c}(\boldsymbol{I} + (\boldsymbol{v}^{t_c})^T\boldsymbol{V}_{t-1}^{-1}\boldsymbol{v}^{t_c})^{-1}(\boldsymbol{v}^{t_c})^T\boldsymbol{V}_{t-1}^{-1}\right]$$

It should be noticed that, $\boldsymbol{v}$ is a $m \times 1$ vector, $\boldsymbol{R}$ and $\boldsymbol{V}$ are $m \times m$ matrix. So $\boldsymbol{I} + (\boldsymbol{v}^{t_c})^T\boldsymbol{V}_{t-1}^{-1}\boldsymbol{v}^{t_c}$ is a scalar, then

$$
\begin{aligned}
\boldsymbol{R}_t^{-1} &= L\boldsymbol{V}_{t-1}^{-1} - \frac{L\boldsymbol{V}_{t-1}^{-1}\boldsymbol{v}^{t_c}(\boldsymbol{v}^{t_c})^T\boldsymbol{V}_{t-1}^{-1}}{1 + (\boldsymbol{v}^{t_c})^T\boldsymbol{V}_{t-1}^{-1}\boldsymbol{v}^{t_c}} \\
&= \frac{L}{L-1}\boldsymbol{R}_{t-1}^{-1} - \frac{L}{L-1}\bullet\frac{\boldsymbol{R}_{t-1}^{-1}\boldsymbol{v}^{t_c}(\boldsymbol{v}^{t_c})^T\boldsymbol{R}_{t-1}^{-1}}{L-1+(\boldsymbol{v}^{t_c})^T\boldsymbol{R}_{t-1}^{-1}\boldsymbol{v}^{t_c}} \quad (25)\\
&= \frac{L}{L-1}\left(\boldsymbol{R}_{t-1}^{-1} - \frac{\boldsymbol{R}_{t-1}^{-1}\boldsymbol{v}^{t_c}(\boldsymbol{v}^{t_c})^T\boldsymbol{R}_{t-1}^{-1}}{L-1+(\boldsymbol{v}^{t_c})^T\boldsymbol{R}_{t-1}^{-1}\boldsymbol{v}^{t_c}}\right)
\end{aligned}
$$

According to above equations, the real time model structure determination procedure can be summarized as Fig. 1.

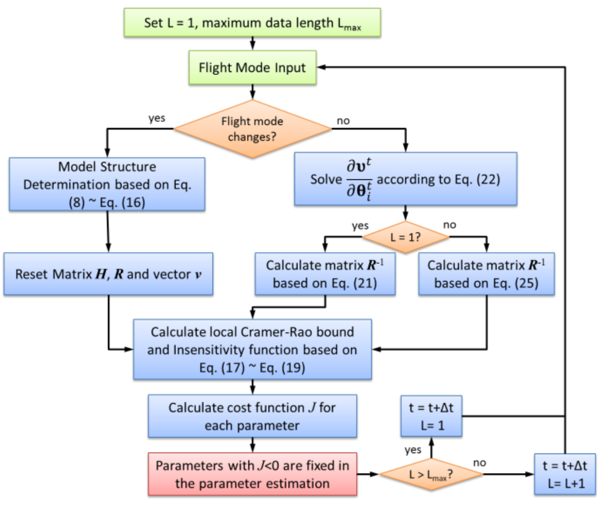

Fig. 1 Real time model structure identification

The maximum data length $L_{\max}$ is used to prevent data saturation problem in calculation of $\boldsymbol{R}^{-1}$. When the data length reaches $L_{\max}$, the covariance matrix is reset based on current model prediction error.

If the cost function is minus for certain model parameter, it means that the overall identification accuracy of this parameter is poor. It also indicates the current measurement data cannot provide sufficient information to modify this parameter. Therefore, it does not need to update the value of this parameter in this step.

The model structure identification is able to select the most sensitive parameters for parameter estimation. The optimal model structure is maintained all the time, and it helps to increase the accuracy of parameter estimation.

3.2. Online parameter estimation

After model structure determination, the remaining problem is online parameter estimation. Considering that the measurement data of tilt-rotor aircraft may be contaminated heavily by unideal measurement noise, a colored noise model is introduced in this paper. Then in order to apply adaptive model structure identification in parameter estimation, an improved weighted recursive least squares algorithm is established.

The colored noise model could be written as Eq. (26).

$$\boldsymbol{\varepsilon}(t) = \boldsymbol{\xi}(t) + \boldsymbol{d}_1\boldsymbol{\xi}(t-\Delta t) + \boldsymbol{d}_2\boldsymbol{\xi}(t-2\Delta t) \quad (26)$$

Where, $\boldsymbol{\varepsilon}$ is colored noise vector, $\boldsymbol{\xi}$ is noise description vector which can be approximated by model prediction error, $\boldsymbol{d}_1$ and $\boldsymbol{d}_2$ are noise model parameter vector, Δt is sampling time interval.

Combine Eq.(8) and Eq. (26), a regress model for parameter estimation can be obtained as Eq. (27).

$$\boldsymbol{y}(t) = \boldsymbol{h}^T(t)\boldsymbol{\theta} + \boldsymbol{\xi}(t) \quad (27)$$

Where, $\boldsymbol{y}$ is output vector, $\boldsymbol{h}$ is regression matrix which has the form as Eq. (28).

$$\boldsymbol{h}^T(t) = \begin{bmatrix}
\boldsymbol{x}^T(t) & \boldsymbol{u}^T(t) & \xi_1(t-\Delta t) & \xi_1(t-2\Delta t) & 0 & 0 & 0 & 0 & \cdots & \cdots & \cdots & \cdots & 0 \\
\boldsymbol{0} & \boldsymbol{0} & 0 & 0 & \boldsymbol{x}^T(t) & \boldsymbol{u}^T(t) & \xi_2(t-\Delta t) & \xi_2(t-2\Delta t) & 0 & 0 & \cdots & \cdots & 0 \\
\vdots & \vdots & \vdots & \vdots & \vdots & \vdots & \vdots & \vdots & \ddots & 0 & \cdots & \cdots & 0 \\
\boldsymbol{0} & \boldsymbol{0} & 0 & 0 & \boldsymbol{0} & \boldsymbol{0} & 0 & \cdots & 0 & \boldsymbol{x}^T(t) & \boldsymbol{u}^T(t) & \xi_m(t-\Delta t) & \xi_m(t-\Delta t)
\end{bmatrix} \quad (28)$$

In which, $\boldsymbol{x}$ is state vector, $\boldsymbol{u}$ is control input vector. The dimension of $\boldsymbol{x}$ and $\boldsymbol{u}$ can be determined according to Eq. (9) and (10).

Presented at 44th European Rotorcraft Forum, Delft, The Netherlands, 19-20 September, 2018

Then parameter estimation in each sampling time can be done by using Eq. (29).

$$(29)\ \begin{cases} \hat{\theta}(t) = \hat{\theta}(t-\Delta t) + \boldsymbol{Q}(t)\boldsymbol{K}(t)[\boldsymbol{y}(t) - \boldsymbol{h}^T(t)\hat{\theta}(t-\Delta t)] \\ \boldsymbol{K}(t) = \boldsymbol{P}(t-\Delta t)\boldsymbol{h}(t)\left[\boldsymbol{h}^T(t)\boldsymbol{P}(t-\Delta t)\boldsymbol{h}(t) + \boldsymbol{I}\right]^{-1} \\ \boldsymbol{P}(t) = \left[\boldsymbol{I} - \boldsymbol{K}(t)\boldsymbol{h}^T(t)\right]\boldsymbol{P}(t-\Delta t) \end{cases}$$

Where, $\boldsymbol{P}$ can be defined as Eq. (30), $\boldsymbol{Q}$ is model structure weighting matrix.

$$(30)\ \boldsymbol{P}(t) = \left(\boldsymbol{h}(t)\bullet\boldsymbol{h}^T(t)\right)^{-1}$$

Matrix $\boldsymbol{Q}$ is a $n \times n$ diagonal matrix, and n is current dimension of $\boldsymbol{\theta}$ vector. The values of the diagonal elements in $\boldsymbol{Q}$ can be determined by Eq. (31), and these values will only be 1 or 0. So the introduction of this weighting matrix has no influence on the computational efficiency of original recursive least squares algorithm.

$$(31)\ \boldsymbol{Q}_{ii}(t) = \begin{cases} 1, & if\ J_i(t) > 0, \quad i = 1, 2, \cdots, n \\ 0, & if\ J_i(t) \le 0, \quad i = 1, 2, \cdots, n \end{cases}$$

The final online parameter estimation algorithm can be described by Fig. 2.

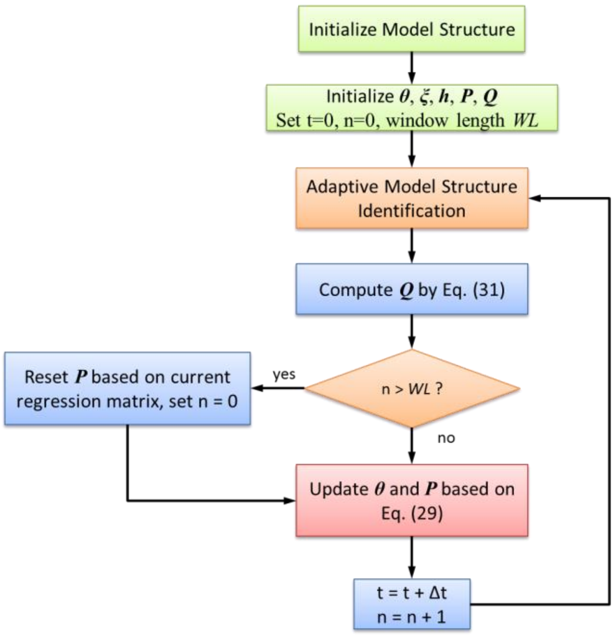

Fig. 2 Online parameter estimation algorithm

The same as in model structure identification, a window with length WL is used to solve the data saturation problem in online system identification. When the data length reaches WL, the covariance matrix $\boldsymbol{P}$ will be calculated according to current regression matrix by Eq. (30).

4. APPLICATIONS TO TILT-ROTOR AIRCRAFT MODEL IDENTIFICATION

The developed online system identification method is firstly applied to a sample tilt-rotor aircraft based on a nonlinear simulation programme. The basic simulation environment is shown in Fig. 3.

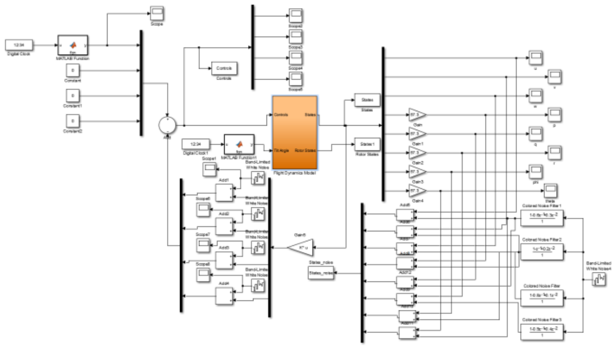

Fig. 3 Simulation environment of tilt-rotor aircraft

Because the tilt-rotor aircraft is an unstable system, so a feedback control system is used to stabilize the aircraft. In order to eliminate high correlations in different control input signals which is usually caused by feedback control system, different white noise signals were added in each control channel. Moreover, in order to consider the influences of unideal noise, different colored noise models were introduced to contaminate the output data in Fig. 3.

Identification were conducted in helicopter mode, transition mode and fixed wing mode based on the simulated flight test. Table 1 shows some of the main derivatives identified by the established identification method in helicopter mode (hover). In order to check the improvements of this paper's method, identification results based on conventional recursive least squares (RLS) method are also listed in the table. The comparison shows that, the overall identification accuracy of this paper's method is better than conventional RLS method, especially for those derivatives in the channel with low signal to noise ratio. This can be further proven by Fig. 4. The prediction error of the identified model using this paper's method is smaller than that based on RLS method. In vertical channel, the signal to noise ratio is very low, the difference between the two identified models is quite obvious. For conventional RLS method, there is no noise model, and the noise is treated as white noise. Therefore, the predicted w (vertical speed in body axis) curve is quite smooth. Moreover, an obvious bias in this curve can be found due to white noise assumption. However, in this paper's method, the colored noise is well modelled, so the noise signal

Presented at 44th European Rotorcraft Forum, Delft, The Netherlands, 19-20 September, 2018

is also well predicted and the bias in predicted w curve is also eliminated. The identified parameters of colored noise model are shown in Table 2. The identification accuracy is satisfactory too.

Table 1 Identification results in helicopter mode

Derivatives	True Value	Identified in this paper	Identified by RLS method
X_u	-0.023	-0.021	-0.019
X_w	0.025	0.023	0.012
X_p	-0.078	-0.083	-0.091
X_q	0.856	0.861	0.796
$X_{\beta 1c}$	10.76	9.35	8.86
$X_{\delta long}$	-0.051	-0.058	-0.061
$X_{\delta col}$	0.0296	0.0321	0.0357
Y_v	-0.047	-0.045	-0.049
Y_p	-0.525	-0.517	-0.538
Y_q	-0.109	-0.121	-0.125
$Y_{\beta 1s}$	-10.76	-9.47	-9.13
$Y_{\delta lat}$	0.0287	0.0295	0.0276
Z_w	-0.2931	-0.285	-0.219
Z_q	0.11	0.162	0.371
$Z_{\delta col}$	-0.241	-0.223	-0.183
L_u	0.25	0.217	0.192
L_v	-0.135	-0.128	-0.173
L_p	-3.551	-3.625	-3.387
L_q	-2.272	-2.585	-2.032
$L_{\beta 1s}$	-22.38	-20.334	-18.871
$L_{\delta lat}$	0.1334	0.1567	0.1681
M_u	0.012	0.009	0.005
M_w	0.0066	0.0053	0.0041
M_q	-0.8161	-0.823	-0.785
$M_{\beta 1c}$	-8.257	-8.16	-7.97
$M_{\delta long}$	0.0335	0.0345	0.0318
N_v	0.032	0.031	0.045
N_p	-0.1013	-0.096	-0.087
N_r	-0.3342	-0.3152	-0.2993
$N_{\delta ped}$	0.114	0.109	0.1071

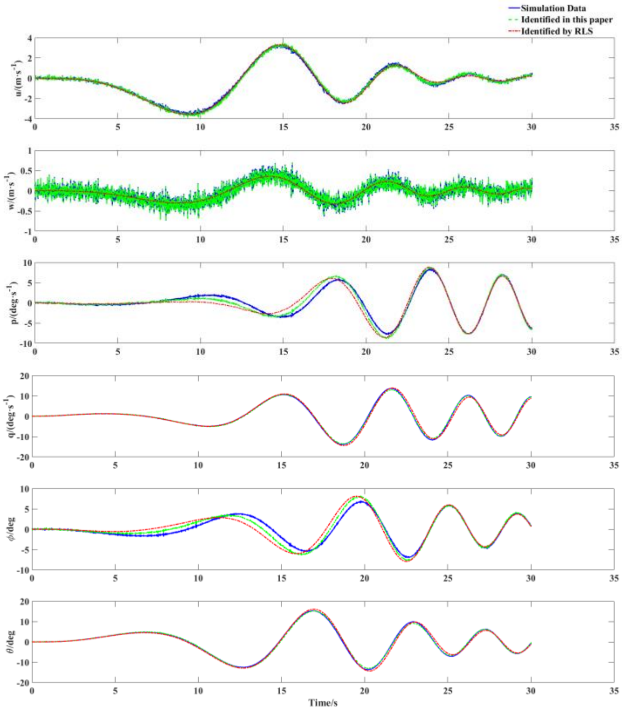

Fig. 4 Verification of identified model in helicopter mode

Table 2 Identification results of noise parameters

Parameters	True Value	Identified Value
$\boldsymbol{d}_{11}$	0.6	0.51
$\boldsymbol{d}_{12}$	0.3	0.17
$\boldsymbol{d}_{21}$	1.0	0.98
$\boldsymbol{d}_{22}$	0.2	0.12
$\boldsymbol{d}_{31}$	0.8	0.76
$\boldsymbol{d}_{32}$	0.1	0.006
$\boldsymbol{d}_{41}$	1.0	0.87
$\boldsymbol{d}_{42}$	0.2	0.13
$\boldsymbol{d}_{51}$	0.6	0.57
$\boldsymbol{d}_{52}$	0.3	0.121
$\boldsymbol{d}_{61}$	0.9	0.88
$\boldsymbol{d}_{62}$	0.4	0.29
$\boldsymbol{d}_{71}$	1.0	0.91
$\boldsymbol{d}_{72}$	0.2	0.13
$\boldsymbol{d}_{81}$	0.6	0.55
$\boldsymbol{d}_{82}$	0.3	0.22

In transition mode, additional control derivatives were identified, Table 3 shows the identification results of pylon derivatives, and Fig. 5 shows the verification results in this flight mode. In order to maintain stability in this flight mode, very small perturbation control signal was applied. Therefore, noise signal is removed in the simulation procedure to ensure the response signal could provide sufficient information for model identification.

Table 3 Pylon derivatives identification results

Parameters	True Value	Identified Value
$X_{\beta p}$	0.306	0.289
$Z_{\beta p}$	0.285	0.238
$M_{\beta p}$	0.016	0.011
$N_{\beta p}$	0.012	0.009

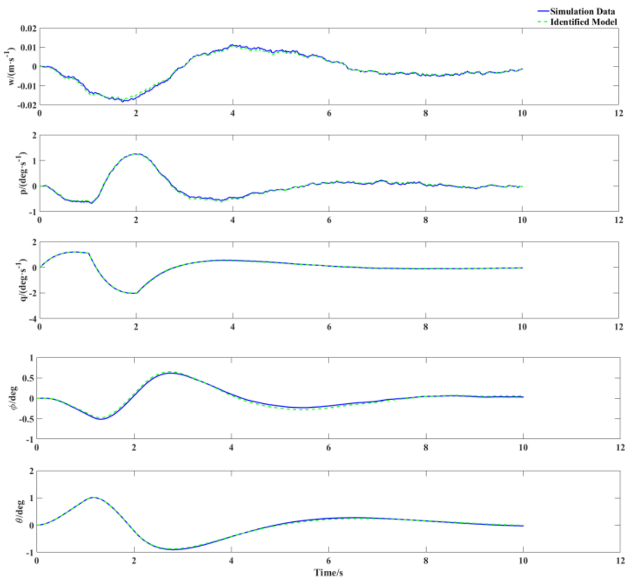

Fig. 5 Verification of identified model in transition mode

Finally, the flight dynamics model of tilt-rotor aircraft in fixed wing mode was identified. Fig. 6 gives the verification results. Because the model is weak coupled in fixed wing mode, the model structure is simpler than those in helicopter and

Presented at 44th European Rotorcraft Forum, Delft, The Netherlands, 19-20 September, 2018

transition mode, so the identification accuracy is even higher in this flight mode.

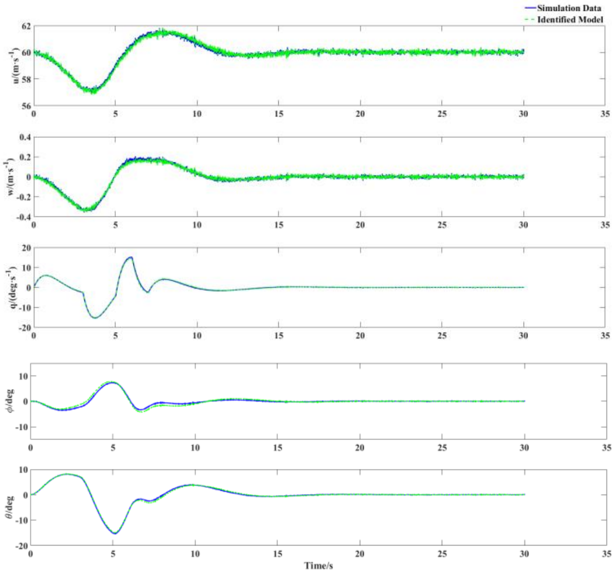

Fig. 6 Verification of identified model in fixed-wing mode

The identification results based on simulation flight test indicate the developed real time identification method works well. It can identify the flight dynamics mode of tilt-rotor aircraft with sufficient accuracy in every flight modes. However, it still needs real flight test data to verify the effectiveness of this method.

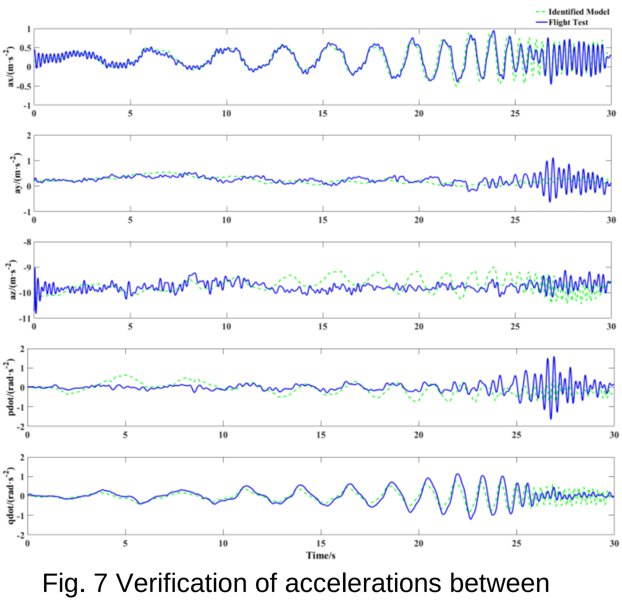

Fig. 7 Verification of accelerations between identified model prediction and flight test data in hover state

A model scale tilt-rotor aircraft is used for identification data generation flight test. Since the transition mode is quite unstable and dangerous, the flight test was only carried out in helicopter hover state. Several groups of frequency sweep excitations were applied to the test aircraft. One group of test data was used for identification, the rest data were used for verification. Fig. 7 and Fig. 8 show the verification results.

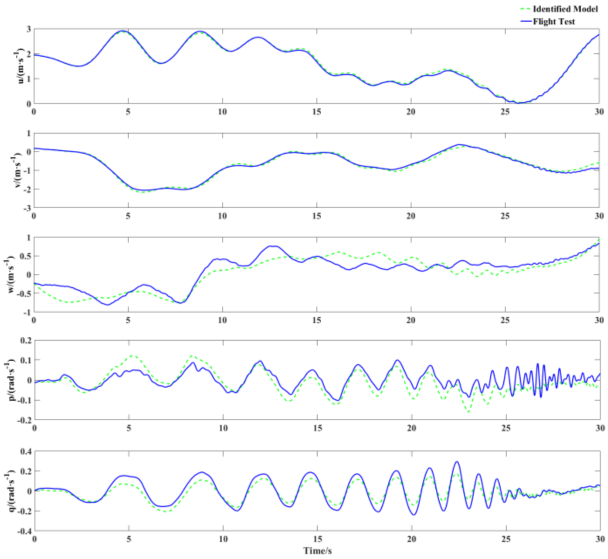

Fig. 8 Verification of states responses between identified model prediction and flight test data in hover state

5. CONCLUSIONS

An improved real time identification method for tilt-rotor aircraft is developed in this paper. The main achievements are summarized as follows:

1) A general weighted time variant linear state space model is established for tilt-rotor aircraft. This model can be used in helicopter mode, transition mode as well as fixed wing mode. The benefit of this general model is a unified identification procedure can be obtained in all flight conditions.

2) An adaptive model structure identification algorithm is developed. A cost function based on local Cramer-Rao bound and Insensitivity function is established to implement model structure identification in real time. Therefore, the optimal model structure is maintained all the time during parameter estimation procedure.

3) Improved online parameter estimation algorithm is developed. Colored noise model is introduced to eliminate parameter estimation bias caused by white noise assumption which is usually applied in conventional online parameter estimation procedure. A weighted recursive least squares algorithm is established to combine the parameter estimation with adaptive model structure identification. The comprehensive identification method shows good identification

Presented at 44th European Rotorcraft Forum, Delft, The Netherlands, 19-20 September, 2018

accuracy for both aircraft parameters as well as noise parameters.

6. REFERENCES

[1] Martin D. Maisel, Demo J. Giulianetti, Daniel C. Dugan. The History of the XV-15 Tilt Rotor Research Aircraft: From Concept to Flight. NASA SP-2000-4517, 2000.

[2] Shao Ming. BA609 Civil Tilt-Rotor Aircraft. Helicopter Technique, 2003, No. 4: 46-52.

[3] Johnson W., Yamauchi G K. NASA Heavy Lift Rotorcraft Systems Investigation. NASA TP-2005-213467, 2005.

[4] Rolf T. Rysdyk, Anthony J. Calise. Adaptive Model Inversion Flight Control for Tilt-Rotor Aircraft. Journal of Guidance, Control and Dynamics. 1999, 22(3):402-407.

[5] Carlos A. Malpica, Colin R. Theodore, Ben Lawrence, James Lindsey, Chris L. Blanken. Handling Qualities of a Large Civil Tilt-Rotor in Hover using Translational Rate Command. American Helicopter Society 68th Annual Forum, Fort Worth, TX, 2012.

[6] Yih Tang Yeo, Hugh H. T. Liu. Transition Control of a Tilt-Rotor VTOL UAV. AIAA Guidance, Navigation and Control Conference. Kissimmee, Florida, 2018.

[7] Carmeron Neil, Padfield Gareth D. Tilt Rotor Pitch/Flight - Path Handling Qualities. Journal of the American Helicopter Society. 2010, 55(4):420-428.

[8] Jung Yong Su, You Ju Yeol, Kwon Oh Joon. Numerical Investigation of Prop-rotor and Tail-wing Aerodynamic Interference for a Tilt-rotor UAV Configuration. Journal of Mechanical Science and Technology. 2014, 28(7):2609-2617.

[9] Hammel P. Rotorcraft System Identification. AGARD-LS-178, 1991.

[10] JRavindra Jategaonkar, Dietrich Fischenberg, Wolfgan von Gruenhagen. Aerodynamic Modeling and System Identification from Flight Data—Recent Applications at DLR. Journal of Aircraft, 2004, 41(4):681-691.

[11] Eugene A. Morelli. Application of System Identification to Aircraft at NASA Langley Research Center. Journal of Aircraft, 2005, 42(1):12-25.

[12] Andrei Dorobantu, Austin Murch, Berenice mettle, Gary Balas. System Identification for Small, Low-Cost, Fixed-Wing Unmanned Aircraft. Journal of Aircraft, 2013, 50(4):1117-1130.

[13] Damiano Rotondo, Fatiha Nejjari, Vicenc Puig. Qusi-LPV Modeling, Identification and Control of a Twin Rotor MIMO System. Control Engineering Practice. 2013, 21:829-846.

[14] Wu Wei, Chen Renliang. Set-Membership Identification Method for Helicopter Flight Dynamics Modeling. Journal of Aircraft, 2015, 52(2):553-560.

[15] Mark B. Tischler, Joseph G. M. Leung, Daniel C. Dugan. Frequency-Domain Identification of XV-15 Tilt-Rotor Aircraft Dynamics. AIAA 2nd Flight Testing Conference, Las Vegas, Nevada, 1983.

[16] Tischler M.B., Leung J.G.M., Dugan D.C. Identification and Verification of Frequency-Domain Models of XV-15 Tilt-Rotor Aircraft Dynamics in Cruising Flight. AIAA Journal of Guidance, Control and Dynamics, 1984, 9(4):446-453.

[17] Tischler M.B. Frequency-Response Identification of XV-15 Tilt-Rotor Aircraft Dynamics. NASA TM-89428, 1987.

[18] Tischler M., Rampel, R. Aircraft and Rotorcraft System Identification: Engineering Methods with Flight Test Examples 2nd Edition. AIAA, Reston, VA, 2012.

[19] John Valasek, Wei Chen. Observer/Kalman Filter Identification for Online System Identification of Aircraft. Journal of Guidance, Control and Dynamics, 2003, 26(2):347-353.

[20] Anthony J. Hebert, Sergio Cafarelli, Paul R. Mackin, Jonathan Shaver. Parameter Identification through Adaptive Optimal Estimation. AIAA Modeling and Simulation Technologies Conference, Grapevine, Texas, 2017.

[21] Han-Hsun Lu, Cameron T. Rogers, Vinicius G. Goecks, John Valasek. Online Near Real-Time System Identification on a Fixed-Wing Small Unmanned Air Vehicle. AIAA Atmospheric Flight Mechanics Conference, Kissimmee, Florida, 2018.

[22] P. Chase Schulze, Brian P. Danowsky, Peijie Yang. Real Time Modal Identification of a Flexible Unmanned Aerial Vehicle. AIAA Atmospheric Flight Mechanics Conference, Grapevine, Texas, 2017.

Presented at 44th European Rotorcraft Forum, Delft, The Netherlands, 19-20 September, 2018